JOURNAL OF PLANKTON RESEARCH | VOLUME 33 | NUMBER 7 | PAGES 1119–1133 | 2011

How to effectively sample the plankton size spectrum? A case study using FlowCAM

EVA ÁLVAREZ [1]*, ÁNGEL LÓPEZ-URRUTIA [1], ENRIQUE NOGUEIRA [1] AND SANTIAGO FRAGA [2]

[1]INSTITUTO ESPAÑOL DE OCEANOGRAFÍA. CENTRO OCEANOGRÁFICO DE GIJÓN, 33212 GIJÓN, SPAIN AND [2]INSTITUTO ESPAÑOL DE OCEANOGRAFÍA. CENTRO OCEANOGRÁFICO DE VIGO, 36200 VIGO, SPAIN

*CORRESPONDING AUTHOR: eva.alvarez@gi.ieo.es

Received October 27, 2010; accepted in principle January 20, 2011; accepted for publication January 23, 2011

Corresponding editor: John Dolan

Any technique developed to enumerate plankton must take into account the size structure of the plankton community. Automatic sampling devices must be capable of analysing a minimum number of cells of the largest size to cover the whole size range intended to be sampled effectively. The Flow Cytometer And Microscope (FlowCAM®) has been used in the last decade to estimate the size structure of the plankton community. Few attempts, however, have been made to compare FlowCAM measurements with the results provided by traditional microscopy methods for size-structure estimations. FlowCAM can operate in three working modes: autoimage, fluorescence triggered and side-scatter triggered. Autoimage and fluorescence triggered cannot only count accurately a mono-specific suspension of cells, but they are also useful to estimate the size structure of natural samples. The side-scatter-triggered mode is not effective to estimate the size structure of natural samples, although it can count a sparse mono-specific solution accurately. The analysis of natural samples with FlowCAM requires a planned pre-processing of the samples to adjust the density of triggering particles (concentrating or diluting the sample) and to pre-filtrate the sample to avoid cell clumping or obstruction of the flow chamber. The size structure obtained with FlowCAM and with microscopy counts on preserved samples are comparable. Sample preservation, however, alters the size structure of the sample, which suggests that results based on preserved samples must be taken with caution. Automatic sampling devices like FlowCAM could provide a more precise analysis of plankton communities, increasing the resolution of surveys and avoiding the effects of preservation and sample storage.

KEYWORDS: FlowCAM; light microscopy; community structure; size spectra; natural populations; sample preservation

INTRODUCTION

The variability of planktonic organisms occurs over a wide range of scales, from centimetres to basin-scales and from hours to decades (Haury *et al.*, 1978). Characterizing these patterns of variability and understanding their causes and consequences require long-term high-resolution monitoring. Traditional methods for plankton enumeration, identification and sizing are,

doi:10.1093/plankt/fbr012, available online at www.plankt.oxfordjournals.org. Advance Access publication March 1, 2011

however, time-consuming. In the last decades, interest in instruments capable of counting, sizing and identifying plankton automatically has increased (Babin *et al.*, 2005; Benfield *et al.*, 2007). At the cost of sacrificing taxonomic detail, the relatively fast analysis of samples obtained by these instruments substantially increases the potential number of samples that can be processed.

These new methods share with traditional methods for plankton enumeration the need to overcome an intrinsic feature of planktonic ecosystems: particle concentration depends both on the type and status of the ecosystem and, for a given status, on the size of the organisms. Smaller organisms are much more abundant than larger organisms, which results in the fact that when randomly picking a certain number of cells, a large proportion is small-sized whereas only a few are large-sized. This inverse relationship between size and abundance can be described through the normalized abundance size spectra (NASS) where the total abundance of cells is binned in size classes on an octave scale, divided by the width of the classes and plotted against size on a log–log scale (Sheldon *et al.*, 1972; Blanco *et al.*, 1994). The question that arises is, what is the minimum number of cells that must be counted to get a reasonable characterization of the larger particles? Techniques developed to enumerate plankton must be capable of analysing this minimum number of cells in a practical time interval.

The Flow Cytometer And Microscope (FlowCAM®) is one of such automatic sampling devices. It combines the capabilities of flow cytometry, microscopy and image analysis (Sieracki *et al.*, 1998). The FlowCAM counts and photographs particles moving in a fluid flow. To create this flow, the water sample is drawn into the instrument by means of a peristaltic pump. A digital camera photographs the particles as they pass through a prismatic glass chamber mounted on a cell holder in front of a microscope lens. Three working modes can be used with the FlowCAM: autoimage, fluorescence-triggered and side-scatter-triggered modes. The difference between them is in the way the camera is triggered. In the autoimage mode, photographs are taken at a constant rate regardless of the concentration of particles in the sample. The fluorescence-triggered and side-scatter-triggered modes take photographs only when a particle matching a triggering criterion passes through the chamber. This triggering criterion is the presence of fluorescent particles or the scatter of light due to any kind of particles. In the three working modes, after taking the photograph, the software extracts each particle present in it, a process named image segmentation. It also records the size and shape information for each particle. The user can then select those particles that match a given criteria, for example a size range or fluorescence level.

The analysis of samples by FlowCAM has been used with several aims, such as the measurement of culture concentration in experimental studies or the estimation of biomass and size–frequency distribution of autotrophic or heterotrophic plankton in natural samples (Table I). Several studies have tested the sizing accuracy of FlowCAM (Sieracki *et al.*, 1998; Sterling *et al.*, 2004; Tauxe *et al.*, 2006) and all have shown that the FlowCAM can properly measure the size of the particles. Some authors have also verified the accuracy of FlowCAM estimates of abundance by comparison against traditional microscopy counts for monocultures, mixed cultures and natural samples (Table I). These comparisons, however, have been done over a limited size range and we lack a formal validation of the capability of the FlowCAM to estimate the size structure of natural plankton communities.

The characteristic flow and particle detection system of the FlowCAM makes it very sensitive to the concentration of particles in the sample being processed. This is supposed to impose important constraints on the size range that is effectively sampled in a given amount of time. The minimum number of cells counted to cover a given size range can saturate the instrument if they are contained in a very small processing volume, whereas it can increase substantially the time of analysis per sample if they are contained in a large processing volume.

The effects of the size structure of planktonic ecosystems on FlowCAM effectiveness for each of the three working modes has not been specifically addressed in the literature. The sensitivity of the FlowCAM to the concentration of particles being analysed is different for each working mode. While the autoimage mode is very sensitive to low concentrations, triggered modes are affected by high concentrations (Sieracki *et al.*, 1998). Consequently, FlowCAM's ability to count natural samples needs to be checked over realistic concentrations and compared with abundance size spectra determined through traditional microscopy. Microscopy counts are usually carried out on Lugol or formaldehyde preserved samples, while with the FlowCAM it is possible to process fresh samples. The effects of preservation and storage, such as cell losses and shrinkage (Menden-Deuer *et al.*, 2001), must be taken into account to make this comparison (Zarauz and Irigoien, 2008).

The general objective of this work is to assess the reliability of FlowCAM to estimate the size structure of natural samples. To this aim: (i) we have estimated the minimum number of cells to be counted to sample effectively a given size range. (ii) According to factory-defined FlowCAM specifications and depending on the total concentration of particles in the processing sample,

Table I: Literature review of FlowCAM applications

Reference	FlowCAM application	Methodological comparison
Sieracki *et al.* (1998)	Original paper	Comparable results of A and F against LM in mono-cultures
Vaillancourt *et al.* (2004)	Size frequencies of cultures	
Sterling *et al.* (2004)	Sizing of aggregates in aquatic sediments	
Lavrentyev *et al.* (2004)	Abundance of photosynthetic nano-eukaryotes	Comparable results of F against EPM in natural samples (size range: 3–20 μm) but not shown
See *et al.* (2005)	Abundance of micro-plankton	Comparable results of A against EPM in natural samples (>15 μm); not comparable results against LM
Clough and Strom (2005)	Abundance of *Heterosigma akashivo* in cultures	
Liu *et al.* (2005)	Size frequency of micro-plankton	
Tauxe *et al.* (2006)	Size frequency of flocs	
San Martin *et al.* (2006a, 2006b)	Size spectra of nano- and micro-plankton	
Koski *et al.* (2006)	Differentiation of species by fluorescence	
Buskey and Hyatt (2006)	Detection of *Karenia brevis* in cultures mixtures	Comparable results of A against LM in mono-cultures
Breier and Buskey (2007)	Abundance of phytoplankton	
Zarauz *et al.* (2007)	Size spectra of nano- and micro-plankton	
Ide *et al.* (2008)	Abundance of nano- and micro-plankton	Comparable results of F against LM and EPM in natural samples (3–40 μm)
Cotano *et al.* (2008)	Abundance and size structure of micro-plankton	
Zarauz and Irigoien (2008)	Preservation effect on FlowCAM performance	
Littman *et al.* (2008)	Abundance of *Sybiodinium* sp. in coral reefs	Not comparable results of F or S against LM in natural samples (size around 10 μm)
Kudela *et al.* (2008)	Abundance of harmful algae	
Buskey (2008)	Abundance of micro-plankton	
Gribben *et al.* (2009)	Abundance of micro-plankton	
Zarauz *et al.* (2009)	Size spectra of nano- and micro-plankton	
Barofsky *et al.* (2010)	Abundance of protozoa	Comparable results of A against LM in mesocosms (11 m^3, ~30–100 μm) but not shown
Pedersen *et al.* (2010)	Size structure and morphology of plankton community	
Tanoi *et al.* (2010)	Size and image colonies of *Botryococcus braunii*	
Töpper *et al.* (2010)	Visual identification of nano-eukaryotes	
Nielsen *et al.* (2010)	Total and size-fractionated biovolume of phytoplankton	
Reynolds *et al.* (2010)	Particle size distributions	Not comparable results of S against LISST and CC in monocultures and natural samples (15–30 μm)
Brzezinski *et al.* (2010)	Nano- and micro-plankton abundance	Not comparable results (mode not specified) against EPM in microcosms (20 L)
Bauman *et al.* (2010)	Phytoplankton abundance and diversity	

Those works which present results from FlowCAM comparison against other methods are shown: A, F and S stand for autoimage, fluorescence-triggered and side-scatter-triggered FlowCAM working modes. LM, light microscopy; EPM, epifluorescence microscopy; LISST, Laser In Situ Scattering and Transmissometry; CC, coulter counter.

we have converted this minimum number of cells in time of analysis, simulating a FlowCAM-specific relationship between the required time of analysis and the size range effectively sampled. (iii) We have also tested the different counting accuracy of the three FlowCAM working modes, the counting accuracy for samples with a realistic size structure, and whether the FlowCAM is capable of reproducing accurately the size spectrum of a natural sample taking into account the effects of preservation and storage.

METHOD

Effective sampling of the plankton size spectrum

To represent the abundance size spectra of plankton communities, we used the empirical relationship given by Blanco *et al.* (Blanco *et al.*, 1994). They fitted a linear regression to a collection of NASS from different sources (the so-called superspectrum). We used this average "superspectrum" slope to calculate how many particles must be counted to sample effectively the size spectrum from pico- to meso-plankton. We arbitrarily defined that at least 10 particles should be counted to consider a size class to be representatively sampled. A size range from pico- to meso-plankton is too wide to be covered by a single methodology, so we estimated the number of cells to be counted for any possible size range between a lower and an upper size limit, both between 0.2 and 2000 μm. And finally, considering the mean abundance of cells in the ocean given by Blanco *et al.* (Blanco *et al.*, 1994), i.e. the "superspectrum" intercept, we estimated what sea-water volume needs to be collected to count such a representative number of cells.

Case study using FlowCAM: tradeoffs between time of analysis and size range effectively sampled

For the FlowCAM, the limitations in the volume analysed and the maximum concentration of particles impose important constraints on the number of cells, and thus the size range, that is effectively sampled in a given amount of time. In order to better understand these limitations, we conducted a series of simulations to understand the tradeoffs between time of analysis and size range that can be effectively sampled.

We calculated the amount of time necessary to obtain a representative count for a given size range and a given total concentration of particles in the sample within this size range. This representativeness will vary with the size of the particles considered. For the smallest particles, which are relatively more abundant, it will be possible to obtain a representative count in a lower amount of time than for large particles, which are scarcer. We used the average "superspectrum" (Blanco *et al.*, 1994) to simulate the size range that can be effectively sampled by taking into account the total concentration of particles, the size-spectrum slope and time of analysis. This would vary for the size range chosen and for each operating mode.

FlowCAM specifications

The FlowCAM used in this work belongs to the series VS4 and was purchased in 2008. FlowCAMs are provided with several microscope lenses. Each lens has its respective flow chamber and the focal depth of each lens is sufficient to cover the depth of the flow chamber (Sieracki *et al.*, 1998). The depth of the flow chamber sets the upper limit for the size of the particles that can be analysed, while the lower limit is determined by the smaller size resolved by the magnification. In this study, we have examined the performance at ×200, ×100 and ×40 magnifications which have an optimum, factory defined, particle size range of 3–50, 15–100 and 30–300 μm, respectively (Table II).

The digital camera has a resolution of 1024 × 768 pixels. For each magnification, a size calibration constant gives the actual dimensions of the camera field-of-view. This field-of-view is not enough to cover the whole width of the flow chamber (at least for the FlowCAM model we have used). The relation between the total width of the flow chamber and the width of the field-of-view gives the percentage of the sample that is analysed (Pi). The volume sampled in one photograph (Vi) is a prism of dimensions: field-of-view width × field-of-view height × flow-chamber depth.

Table II: General characteristics of FlowCAM, setup for each working mode (autoimage, fluorescence- and side-scatter-triggered modes) and pre-treatment of the samples for the three magnifications (200×, 100× and 40×).

	Magnification		
	×200	×100	×40
General characteristics			
Flow chamber depth (μm)	50	100	300
Lower limit (μm)	3	15	30
Flow chamber width (μm)	1000	2000	3000
Calibration constant (μm pixel^{-1})	0.2953	0.6151	1.6386
Field-of-view width (μm)	302.39	629.86	1677.93
Field-of-view heigth (μm)	226.79	472.4	1258.44
Pi: % sample view	30.24	31.49	55.93
Vi: volume per photo (mL)	3.43×10^{-6}	2.98×10^{-5}	6.33×10^{-4}
Max flow rate (mL min^{-1})	0.053	0.53	1.20
Min flow rate (mL min^{-1})	0.012	0.12	0.25
Max frame rate (photos s^{-1})	11	11	11
Autoimage			
Number of photos	20 000	20 000	10 000
Time of analysis (min)	30	30	33
Frame rate (photos s^{-1})	11	11	5
Flow rate (mL min^{-1})	0.05	0.4	0.5
Triggered modes			
Flow rate (mL min^{-1})	0.04	0.12–0.4	0.4
Time (min)	25	25	25
Pre-treatment			
Filtration (μm)	40	100	200
Concentration (μm)	–	15	15

The final net volume analysed (Vn) depends on the working mode. In the case of autoimage, photographs are taken at a constant frame rate. The frame rate must be low enough to avoid overlapping photos, consequently only a portion of the whole volume passing in front of the camera is photographed. The final Vn in autoimage is therefore calculated as the volume sampled in one photograph (Vi) times the number of photographs taken (frame rate × time of analysis). Both triggered modes take a photograph of every particle matching the triggering criterion, so Vn is the whole volume passing in front of the camera and is equal to the volume pumped through the instrument (flow rate × time of analysis) times the percentage of the sample analysed (Pi). In summary, for a given flow rate, the autoimage mode will analyse a smaller volume than the trigger modes.

The maximum concentration of particles in the sample that the instrument can handle also differs in autoimage and triggered modes. The limitation in autoimage is defined by the capability of the software to discriminate individual particles in the photographs (Sieracki *et al.*, 1998) and of the fluidics system to

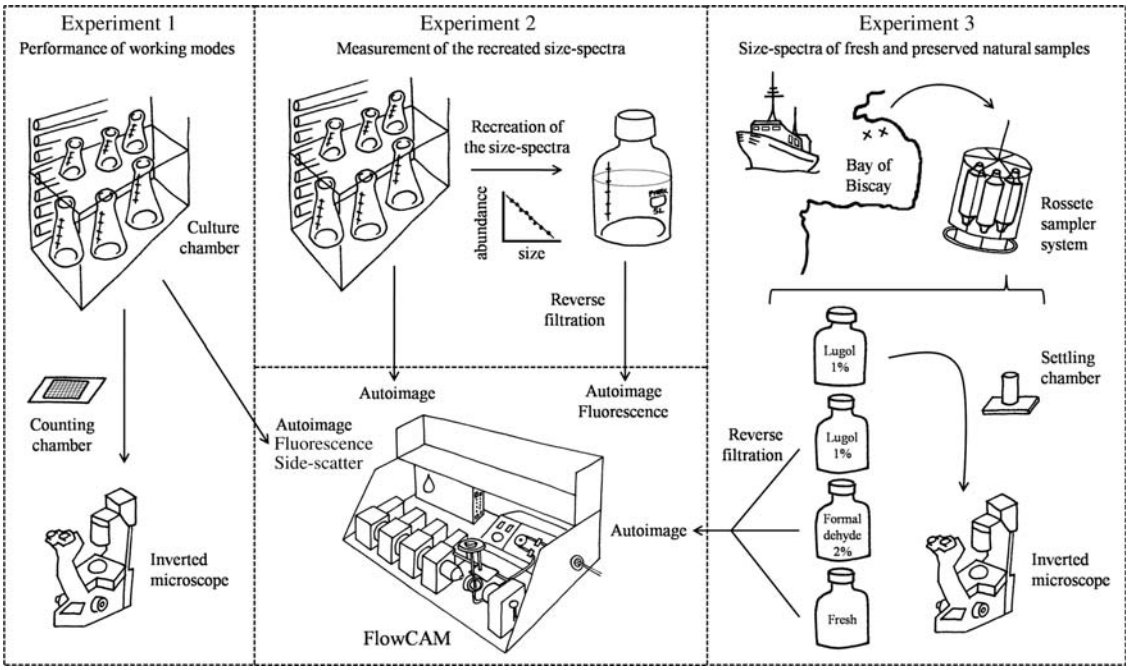

Fig. 1. Schematic representation of the set of experiments carried out to assess the FlowCAM reliability.

maintain all the particles homogeneously embedded in the fluid, avoiding obstructions of the flow chamber or aggregations of particles. For both triggered modes, the limitation is set by the fact that every particle within the size range covered by each lens/flow-chamber combination is capable of triggering the camera but only the particle that caused the trigger should be present in each photograph. In summary, the maximum concentration in triggered modes must be smaller than in the autoimage mode.

Experiments

A set of experiments have been carried out to tackle our objectives and validate the results arising from the simulations. In Experiment 1, we tested the performance of the three FlowCAM working modes using monocultures and latex-bead suspensions at different concentrations. Experiment 2 aimed to check if the FlowCAM is capable of counting accurately a community with a realistic size structure, so we have recreated size spectra with cultures of known concentration and then counted them with the FlowCAM in autoimage and in fluorescence-triggered modes. Finally, in Experiment 3, we compared, for several natural samples, the size spectra determined with FlowCAM, both on fresh and preserved samples, with those obtained using traditional microscopy on the preserved samples (Fig. 1).

General experimental procedures

All samples processed with FlowCAM were pre-filtered through a mesh smaller than the depth of the flow chamber in order to avoid obstructions. Dense samples were diluted with culture media (L1, 32 psu) in Experiment 1 or with filtered sea-water (0.2 μm, 32 psu) in Experiment 2. The samples analysed at 100× and 40× magnifications were concentrated by reverse filtration (Dodson and Thomas, 1978) with a 15 μm mesh (Table II). Although this concentration procedure resulted in some samples being analysed beyond the FlowCAM specification limits, this was done in order to validate the results arising from the simulations. The total number of cells counted was divided by the Vn and multiplied by the dilution factor to determine the cell concentration in the initial sample.

Experiment 1: performance of FlowCAM working modes

Seven phytoplankton cultures were used to test the performance of each of the three working modes. The cultures were obtained from the Toxic Phytoplankton Culture Collection from the Centro Oceanográfico de Vigo (Instituto Español de Oceanografía) and are summarized in Fig. 2 where their images, size and combination magnification/flow chamber used to count them are shown.

To determine the cell concentration in the cultures, an aliquot of 4 mL was fixed with 20 μL of Lugol solution, homogenized and then 1 mL was placed in a Sedgwick-Rafter counting chamber and counted under

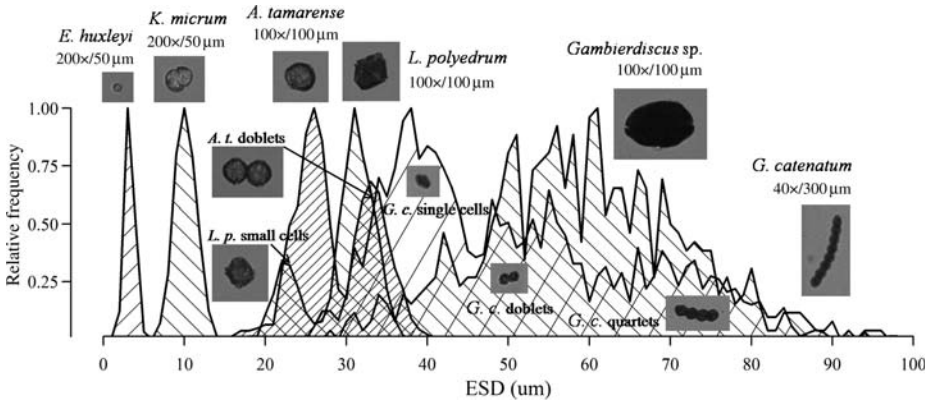

Fig. 2. Relative size frequencies of the seven cultures used in Experiment 1. Only six of them were used to reproduce the min, average- and max-NASS in Experiment 2 (see Table III).

Table III: Abundance (cells L^{-1}) predicted from the empirical NASS given by Blanco et al. *(Blanco* et al., *1994) for each biovolume class*

Bio-volume class (μm^3)	ESD (μm)	Abundance (Blanco *et al.*, 1994)	Species	Abundance min-NASS	Abundance average-NASS	Abundance max-NASS
16	3	2.33×10^5				
32	4	1.19×10^5	*E. huxleyi*	4.13×10^4	4.13×10^5	4.13×10^6
64	5	6.06×10^4				
128	6	3.09×10^4				
256	8	1.57×10^4	*K. micrum*	5.47×10^3	5.47×10^4	5.47×10^5
512	10	8.03×10^3				
1024	13	4.09×10^3				
2048	16	2.09×10^3	*A. tamarense*	724	7.24×10^3	7.24×10^4
4096	20	1.06×10^3				
8192	25	542				
16 384	32	276	*L. polyedrum*	96	960	9.60×10^3
32 768	40	141				
65 536	50	71.8				
131 072	63	36.6	*Gambierdiscus* sp.	13	127	1.27×10^3
262 144	79	18.7				
524 288	100	9.52				
1048 576	126	4.85	*G. catenatum*	2	17	168
2097 152	159	2.47				

The biovolume class is defined by its lower limit, from which the corresponding ESD is also shown. The cultured species used to recreate the size spectra are shown together with their abundances (cells L^{-1}) in each of the three reference size spectra: min-, average- and max-NASS.

a NIKON inverted microscope. Each culture was then diluted and counted again under the inverted microscope following the procedure previously described. The difference between the desired concentration and the actual one was calculated as a manipulation error and was on average 6%.

Each sample was processed with the FlowCAM in triplicate with the specifications shown in Table II. Samples counted with the 100× and the 40× magnifications were analysed in the three working modes. Samples counted with the 200× magnification were analysed only in autoimage and in the fluorescence-triggered mode because the side-scatter detection was unreliable at this magnification in the FlowCAM instrument used. An additional series of experiments with latex beads were conducted to establish the limitations of the side-scatter-triggered mode (see Supplementary Data, Appendix A).

The results were compared to the microscopy counts with a *t*-test (Zar, 1999). Size information from this experiment was used to determine the size–frequency of each culture (Fig. 2) in order to decide which cultures to use in the recreation of the size spectra (Experiment 2).

Experiment 2: measurement of the recreated size spectra

With the regression line given by Blanco *et al.* (Blanco *et al.*, 1994) (normalized abundance = 6.538 − 1.972 × biovolume), we predicted the abundances in each biovolume class for particles between 3 and 200 µm (Table III). The intercept of this regression was

increased and decreased one unit to obtain an upper and a lower limit of abundance, respectively, which means a variation of two orders of magnitude in abundance and encompasses most variability in the data compiled by Blanco *et al.* (Blanco *et al.*, 1994). These three reference size spectra are referred to as min-NASS, average-NASS and max-NASS.

To recreate these reference NASS, we combined six cultures from Experiment 1. *Prorocentrum balticum* was excluded because it was difficult to distinguish from *Karlodinium micrum* by size or morphology (Fig. 2). Each culture represented three biovolume-classes from Blanco *et al.* (Blanco *et al.*, 1994) and the desired concentration was calculated as the sum of these three classes (Table III). The six cultures were kept close to the optimal concentration tested in Experiment 1 in their respective culture flasks growing in L1 culture media with controlled photo-period (14:10 light–dark), irradiance (~90 μmol quanta m^{-2} s^{-1}) and temperature (24 ± 1°C for *Gambierdiscus* sp. and 18 ± 1°C for the rest). Each day, the cultures were counted with the FlowCAM in the autoimage mode taking 10 000 photos with 200× and 100× magnifications and 5000 photos with 40× magnification since our results from Experiment 1 showed that this procedure resulted in reliable counts. Once the six concentrations were known, the culture volumes needed to recreate 5 L of each of the three reference size spectra were calculated. Each day of the experiment, one of the reference size spectra was recreated in filtered sea-water.

Three replicates of each sample were analysed (Table II). Each replicate was processed in autoimage and in the fluorescence-triggered mode with the 200× and 100× magnifications but only in autoimage with the 40× magnification due to malfunction of the fluorescence-triggered mode at this magnification in the FlowCAM used. Cells from each species were separated by visual inspection of the images taken. Only bins with at least 10 counted particles in two of the replicates were included. The parameters of the regression line fitted to the measured NASS were compared with the slope and intercepts of the three reference NASS using a *t*-test (Zar, 1999).

Experiment 3: size spectra of fresh and preserved natural samples

Natural samples were taken with a rosette sampler system at a coastal (46.4219°N, 1.8477°W, 25 m) and a mid-shelf station (45.7943°N, 3.3714°W, 142 m) in the Bay of Biscay. At each site, three replicates, each using a separate Niskin bottle, were taken at the depth of the chlorophyll maximum, 12 and 30 m, respectively.

For each replicate, four 1-L samples were taken. One was kept fresh, stored in the dark and analysed with the FlowCAM in the autoimage mode within the next 12 h. Another was preserved with Lugol solution 1% final concentration and used to count and size microplankton under the inverted microscope. Two litres were preserved with Lugol 1% and formaldehyde 2%, respectively, and analysed with the FlowCAM in the autoimage mode within the next month.

For analysis under the microscope, 25 mL for the coastal and 100 mL for the mid-shelf station were dispensed into Utermöhl settling chambers and the phytoplankton cells were allowed to settle for 24 and 72 h, respectively (Utermöhl, 1958). Chambers were imaged at 100× (two stripes) and 200× (one stripe) using a LEICA inverted microscope equipped with a digital photo-camera. Length and width for each individual organism in the images were measured. The projected area of each particle was calculated based on its shape (rectangle or ellipse) and converted to an equivalent spherical diameter (ESD) comparable with that provided by FlowCAM. The images provided by the FlowCAM were manually classified in order to eliminate non-valid images (detritus, bubbles . . .) in both fresh and preserved samples. The Vn and total number of cells sized with each methodology are summarized in Table IV.

A *t*-test on the NASS calculated for Lugol-preserved samples was applied to compare the size spectra obtained with FlowCAM and traditional microscopy. To compare the effects of preservation, a one-way ANOVA and a Tukey test (Zar, 1999) were applied to the NASS calculated for fresh, and Lugol and formaldehyde-preserved samples analysed with FlowCAM.

Table IV: Net sampled volume (mL) and number of cells counted and sized (between 5 and 20 μm for 200× magnification and 20–100 for 100× magnification) with FlowCAM and microscopy for the two natural samples

Sample	Magnification	Volume FlowCAM	Volume microscope	Sized cells FlowCAM	Sized cells microscope
Mid-shelf	×100	23.8	10.28	33	16
	×200	0.14	2.17	11	104
Coastal	×100	9.84	2.57	750	384
	×200	0.08	0.54	39	243

RESULTS

What is the minimum number of counted cells needed to have a good representation of a given size range?

Figure 3 illustrates the total number of cells that must be counted to cover a given size range and how this number translates in sea-water collected volume. The total number of cells counted is independent of the total concentration of cells in the sample, and only depends on the relative abundance of each size class, i.e. the spectrum slope. Figure 3A shows the total number of cells that must be counted to cover the whole size spectrum from pico-plankton up to an upper limit. For instance, to sample effectively micro-plankton, we must count 6.24×10^9 cells between 0.2 and 200 μm.

However, to consider the total number of cells from pico-plankton to the size object of study seems not very practical. It is more useful to calculate a minimum number of cells within a downward-limited size range. Figure 3B shows the number of counted cells needed to cover a specific size range defined by a lower and an upper limit. Following the example with the micro-plankton, the total number of counted cells between 20 and 200 μm must be 8760 cells within this size range. Note that this number is not the simple difference between the required number of cells for sampling up to 20 μm and the cells for sampling up to 200 μm, but the cells needed for sampling up to 200 μm minus all cells smaller than 20 μm included in this minimum number and correspond to the dashed area in Fig. 3A.

Figure 3C translates the variable counted cells into collected volume considering the mean abundance of cells given by Blanco, i.e. the spectrum intercept. In our example of sampling micro-plankton, the required volume is 4.04 L.

Case study using FlowCAM: tradeoffs between time of analysis and size range effectively sampled

Figure 4 illustrates the results of the simulation obtained for the ×100 magnification and the factory defined size range of 15–100 μm (similar simulations for 200×/3–50 μm and 40×/30–300 μm are shown in Supplementary Data, Figs S1 and S2 and Appendix B). The upper panels (Fig. 4A–C) show how as the concentration of particles increases, the time required to sample effectively decreases. Figure 4D–F shows examples of how these graphs should be interpreted. Taking into account that in natural samples the total concentration of particles in the size range of 15–100 μm is 8 cells per mL according to the "superspectrum" of Blanco *et al.* (Blanco *et al.*, 1994), the time required to sample effectively the whole factory defined size range would be 454 h in the autoimage mode (Fig. 4D) and 54 h in the triggered modes (Fig. 4E). This is achieved at the maximum frame rate of 11 frames per second in the autoimage mode and the maximum flow rate of 0.53 mL min^{-1} in the triggered modes. These graphs are achieved by drawing vertical lines in Fig. 4A and B or C at this concentration of 8 cells per mL and plotting the intersection of this line with the isoclines of upper size range sampled effectively versus time.

In the triggered modes, there is a limitation in the number of events per second that the instrument can handle: 2 and 0.5 events per second in the fluorescence (Sieracki *et al.*, 1998) and side scatter triggered modes (Brown, 2010), respectively (see Supplementary Data, Appendix A). Thus, when the concentration in a sample is so high that this limit is surpassed at the maximum flow rate (above 226 and 57 cells mL^{-1} for fluorescence and side-scatter-triggered modes, respectively), the flow

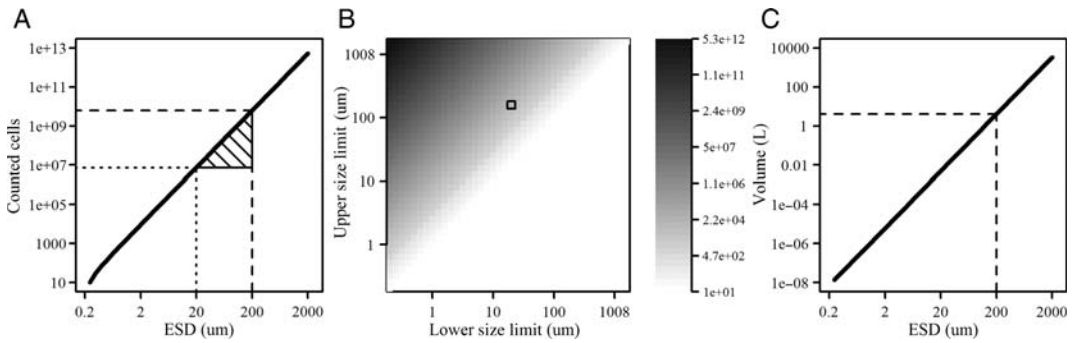

Fig. 3. Minimum number of counted cells needed to have a good representation of a given size range. (**A**) Total number of cells to be counted to sample effectively the size range from pico-plankton up to an upper limit (μm); (**B**) minimum number of cells to be counted to sample effectively a size range defined by a lower and a upper limit (μm); and (**C**) minimum sea-water volume needed to be collected to sample up to an upper limit (μm). Dotted line (A) indicates an example for the sampling up to nano-plankton (0.2–20 μm). Dashed lines (A and C) indicate an example for the sampling up to micro-plankton (0.2–200 μm) and the dashed area (A) and the little square (B) indicates an example for the sampling of micro-plankton (20–200 μm).

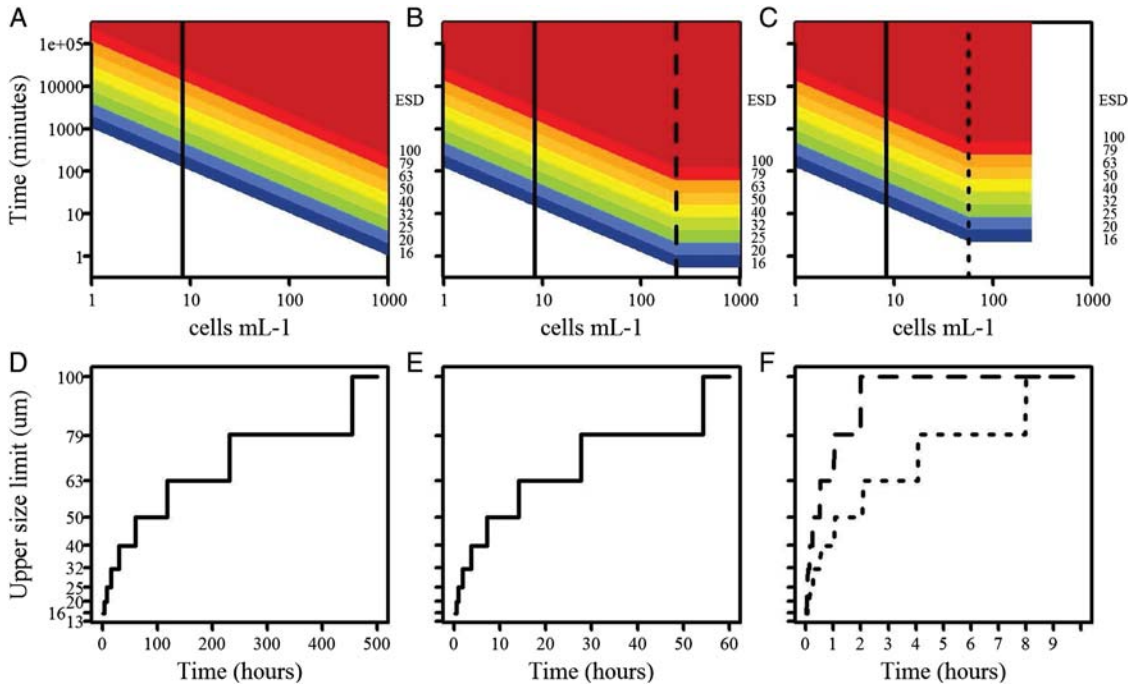

Fig. 4. Simulation for the combination magnification/flow chamber 100 × 100 μm. The upper panels show the upper size limit sampled effectively given the total concentration of particles in the size range of 15–100 μm and the time of analysis for the (**A**) autoimage mode, (**B**) fluorescence-triggered mode and (**C**) side-scatter-triggered mode. The correspondence of each shaded area with the ESD (μm) is indicated in the right axis of each panel. Lower panels show examples of upper size limit sampled versus time for (**D** and **E**) a mean natural sample concentration of 8 cells mL^{-1}, calculated according to Blanco *et al.* (Blanco *et al.*, 1994) and indicated as vertical lines in (A)–(C), for (**D**) autoimage and (**E**) triggered modes. (**F**) shows the same relationship for the concentrations at which the saturation of the triggered modes is reached, indicated as vertical dashed and dotted lines in (B) and (C), respectively.

rate should be reduced. So at concentrations higher than these thresholds, there are no means to reduce the amount of time necessary to sample effectively because the possible events per second is set. This results in the fact that above these threshold concentrations the isoclines in Fig. 4B and C are horizontal and the time required to sample effectively is constant as represented in Fig. 4F: 2 h in fluorescence-triggered and 8 h in side-scatter-triggered modes. However, the flow rate cannot be decreased infinitely so the cell density at which the events per second limit is reached at minimum flow rate sets an overall upper limit for the densities each trigger mode can count accurately (1000 and 250 cells mL^{-1} for fluorescence- and side-scatter-triggered modes, respectively).

Obviously 454 and 54 h is unacceptably long for a sample analysis, which explains the need for concentrating natural samples to obtain reliable estimates of the size spectra. Considering 30 min to be a reasonable amount of time for processing each sample, in the side-scatter mode, the maximum total number of particles that can be analysed in 30 min is 279 (i.e. 30 events per minute times Pi = 0.31). This implies that in 30 min only the size range between 15 and 32 μm can be sampled, even if the sample is concentrated. In the fluorescence mode, this maximum total number of particles that can be analysed in 30 min is 1116 (i.e. 120 events per minute times Pi = 0.31). So in 30 min, it is possible to cover effectively the range between 15 and 50 μm.

Experiment 1: performance of each working mode

The performance in the autoimage mode was good (Fig. 5). The slope of the relationship between autoimage and microscopy counts was 1.038 ± 0.045 ($R^2 = 0.9648$, P-value < 0.0001, $n = 21$), not significantly different to the 1:1 line (P-value $= 0.4163$). The average percentage error, calculated as the absolute difference between FlowCAM and microscopy counts relative to the microscopy counts, was 14.8%. As an index of the reproducibility of the counts, we calculated the coefficient of variation within the three replicates for each culture. The average coefficient of variation in the autoimage mode was 12.4%.

In the fluorescence-triggered mode, the relationship had a slope of 0.905 ± 0.030 ($R^2 = 0.9824$, P-value $<$ 0.0001, $n = 18$) not statistically different from the 1:1

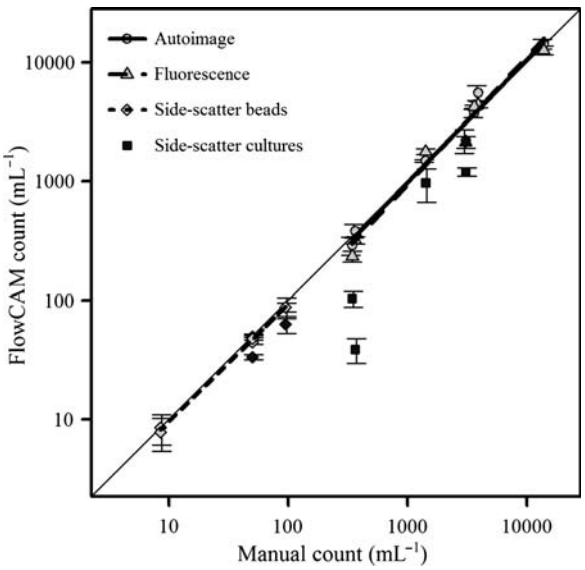

Fig. 5. FlowCAM counting accuracy. Comparison between microscopy and FlowCAM counts for seven different phytoplankton cultures in the three FlowCAM working modes and three latex beads solutions in the side-scatter-triggered mode. Solid thin line shows the 1:1 relationship. The dark triangle and dark rectangles represent points not included in the comparison because they did not meet the factory defined settings.

relationship (P-value = 0.0528). The average percentage error in the fluorescence-triggered mode was 18.1% and the average coefficient of variation was 6.6%. One of the samples had a concentration that was too high for this mode and was analysed at an events per second rate above FlowCAM specifications. As expected, this point fell below the 1:1 line and if included in the calculations caused the slope to be statistically different from 1 (P-value = 0.0231, $n = 21$).

In the side-scatter-triggered mode, the relationship considering only those samples processed under 0.5 events per second (experiment using bead solutions, see Supplementary Data), within the factory specifications for this triggered mode, had a slope of 0.9243 ± 0.044 ($R^2 = 0.9579$, P-value < 0.0001, $n = 21$) marginally statistically different to the 1:1 relationship (P-value = 0.010). The percentage error was on average of 5.6% and an average coefficient of variation of 14.8%. The performance with the other samples exceeding the events per second limitation was poor, with a percentage of error on average of 53.0%.

Experiment 2: measurement of the recreated size spectra

FlowCAM sizing capability is a useful tool to analyse the size–frequency of the samples and we have used it to decide which cultures to include in our simulated size spectra (Fig. 2). The size–frequency distributions of *Emiliana huxleyi*, *K. micrum* and *Gambierdiscus* sp. were unimodal, *Alexandrium tamarense* and *Lygulodinium polyedrum* distributions were bimodal, caused by the presence of doublets and two separate sizes, respectively, and *Gymnodinium catenatum* shows three modal peaks given its appearance in single cells, doublets, quartets and even octets, a consequence of its division mechanism. The size distributions were overlapped which forced the experimental design to use each culture to represent one bin of the recreated size spectra and not to use the biovolume of the particles to build the NASS (Table III).

To cover the size range of 3–200 μm, each of the three recreated NASS was analysed with the three magnifications. Those bins with less than 10 counted particles because of the relative low volume analysed result in curvature of the spectrum and were not included as they could cause potential error in the calculation of the parameters. For instance, bin 6 represented by *G. catenatum* was not properly sampled in any of the three size spectra due to the low volume analysed.

According to this representativeness criterion, the bins properly sampled in the autoimage mode were: 1 (*E. huxleyi*), 3 (*A. tamarense*) and 4 (*L. polyedrum*) for the min-NASS; 1, 3, 4 and 5 (*Gambierdiscus* sp.) for the average-NASS; and from 1 to 5 for the max-NASS

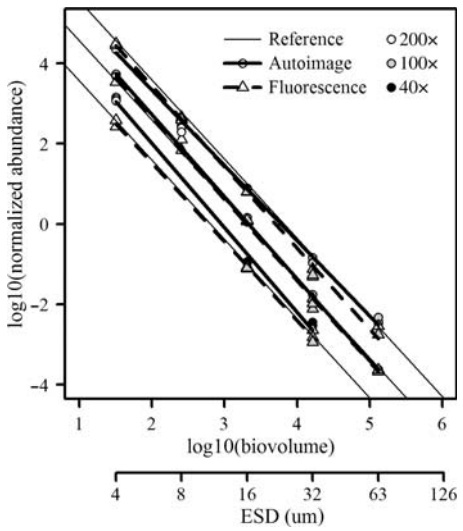

Fig. 6. Measurement of the recreated size spectra. NASS obtained with FlowCAM in the autoimage (solid line) and fluorescence-triggered modes (dashed line) sampling the three recreated spectra, min-, average- and max-NASS (solid thin lines). Each sample was analysed as the combination of three subsamples: 200× (white), 100× (gray) and 40× (black). In the x-axis, in addition to $\log_{10}$(biovolume), the geometric mean of the ESD covered by each sampled bin is shown.

(Fig. 6). Bins number 2 (*K. micrum*) (the larger size class analysed at 200× magnification) and 5 (the larger size class analysed at 100× magnification) were not adequately sampled because the time of analysis (net volume analysed) was too short (low) to obtain representative counts, in accordance with the simulation experiments. Taking into account only those bins that were representatively sampled, the autoimage mode can reproduce accurately the three reference NASS (Fig. 6; min-NASS: P-value = 0.0606, $n = 9$; mean-NASS: P-value = 0.7055, $n = 12$; max-NASS: P-value = 0.2113, $n = 15$).

In the fluorescence-triggered mode, the bins that were properly sampled were 1, 3 and 4 for the min-NASS and from 1 to 5 for the average-NASS (Fig. 6). Taking into account these bins, the fluorescence-triggered mode can reproduce accurately the reference min- and average-NASS (P-value = 0.1946, $n = 8$; P-value = 0.3529, $n = 14$). However, for the max-NASS, which was analysed at a trigger rate higher than 2 events per second, the measured size spectrum was significantly different from the reference NASS (P-value < 0.0001, $n = 14$).

Experiment 3: size spectra of fresh and preserved natural samples

When analysing fresh and preserved samples (Lugol or formaldehyde) with FlowCAM in the autoimage mode, the spectra were significantly different (mid-shelf station: P-value < 0.001, $n = 44$, Fig. 7B–D; coastal station: P-value < 0.001, $n = 101$, Fig. 7F–H). The size-spectrum slope was higher in the fresh samples compared to the preserved samples due to an underestimation of the abundance of small cells and an overestimation of the abundance of the medium-sized particles in the preserved samples. The variance of the NASS bins was larger in the preserved samples than in the fresh samples.

When comparing FlowCAM and microscopy on preserved samples, using only those size bins sampled by both methods, there were no significant differences in the size-spectrum slopes in the mid-shelf sample (P-value = 0.111, $n = 31$, Fig. 7A and C), but significant differences in the coastal one (P-value < 0.001, $n = 81$, Fig. 7E and G). It must be taken into account, however, that the size ranges covered by each method do not overlap completely. The lower limit of detection was 3 μm for FlowCAM and 5 μm for the microscope technique. The upper limit was determined by the net volume sampled (Table IV), 32 μm in the mid-shelf sample and 100 μm in the coastal station. In the coastal samples, although the sampled volume was representative (Table IV), the FlowCAM did not sample the last size class (Fig. 7F–H).

Another difference between microscopy and FlowCAM methods is that the former can sample the size spectra continuously from the lower to the upper limit, while the later does not sample several bins in the middle of the size range, one in the coastal sample and

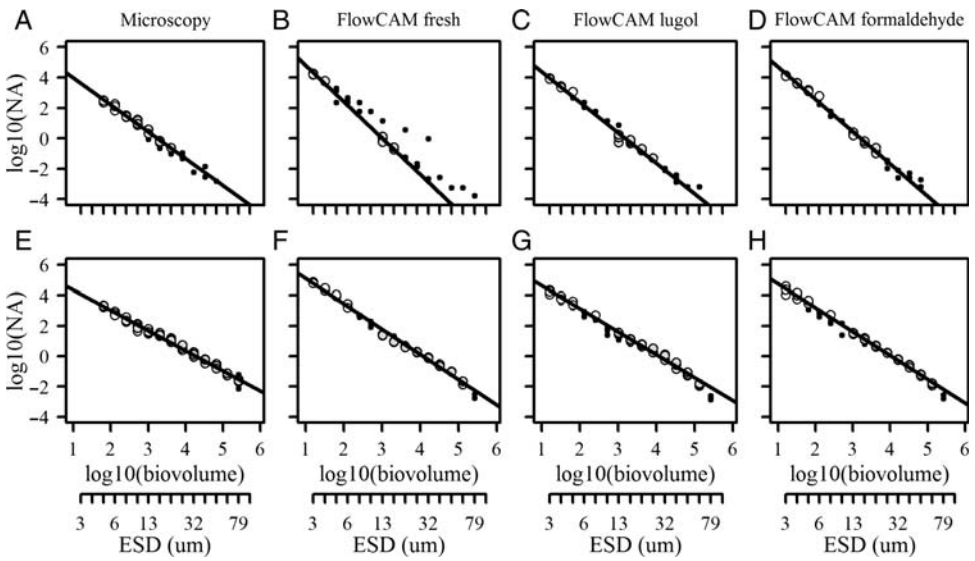

Fig. 7. NASS obtained with microscopy and FlowCAM with different preservation techniques. The upper panels (**A**–**D**) correspond to the mid-shelf sample and the lower panels (**E**–**H**) to the coastal sample. The sample analysed with microscopy was preserved only with lugol solution, whereas the fresh sample and two preservation treatments (lugol and formaldehyde) were examined with FlowCAM. Each sample was analysed as the combination of two subsamples: 200× (white) and 100× (grey). In the x-axis, in addition to $\log_{10}$(biovolume), the min ESD of each sampled bin is shown. Size bins with less than 10 cells imaged are included in the representation (•) but not in the regression analysis.

three in the mid-shelf sample. The un-sampled bins are due to the low volume analysed with the 200× (Table IV). As a consequence, there were few bins in common to compare the size spectra obtained with microscopy and FlowCAM in the mid-shelf sample reducing the power of the statistical test. From the simulations, it is possible to calculate that the additional time necessary to fill the gap with the 200× would be 911 min in the mid-shelf sample and 45 min in the coastal one. The time of analysis in the side-scatter-triggered mode would has been 139 and 22 min, respectively.

DISCUSSION

We have described the scenario in which any plankton sampling methodology must operate, in terms of counted cells and sampled volume. We have then tested the capacity of FlowCAM to work within these limits describing its specific tradeoff between time of analysis and size range effectively sampled.

The main concern when using automatic sampling devices is whether they provide reliable results. For this reason, we have tested the accuracy of FlowCAM in estimating the size structure of natural samples against the results obtained with light microscopy, the traditional method for plankton enumeration and sizing. As long as the factory-defined limitations are considered, our results show that the three working modes can provide accurate abundance estimates. Phytoplankton cultures or latex bead suspensions with concentrations within the factory-defined limits were measured accurately, whereas the suspensions with concentrations beyond the limits were not (Fig. 5). Some studies have reported poor performance of FlowCAM compared with other methodologies (Table I), but it appears that they operate the FlowCAM outside the factory-defined limits (Reynolds *et al.*, 2010).

When the purpose is to reproduce the size spectra (Fig. 6), it is necessary to count enough cells in each size class. We have defined an arbitrary value of 10 sampled cells as the minimum to consider a size class to be effectively sampled. We consider it important to establish this representativeness criterion because a size bin sampled only with a couple of cells can potentially bias the size-spectrum estimation. Our simulations to calculate the size range of particles effectively sampled by each magnification/flow-chamber combination are based on factory-defined parameters (Table II), so they can be reproduced before experimental work to identify the required processing time and sample concentration protocol.

The first point that arises from the simulation is the need to analyse the same sample using several magnification/flow-chamber combinations to cover the complete size spectra. The second point is the necessity to concentrate natural samples in some of the magnification/flow-chamber combinations, because the time of analysis required to estimate the complete size spectra is too high for routine work. The need to concentrate the sample also depends on the status of the ecosystem. For example in Fig. 7, at the coastal site, the 3–15 μm size range is effectively sampled by the ×200 magnification without the need for concentration, but in the mid-shelf sample concentration was required. For micro-plankton, the sample will always require concentration due to their relative low concentration in natural systems.

The degree of sample concentration required will depend on the chosen working mode. In autoimage, the sample can be concentrated up to the limitations imposed by the software and the fluidics (i.e. segmentation of the images and homogeneous distribution of particles in the fluid). These limits are sufficiently high to permit the concentration of natural samples and their accurate analysis in less than 30 min.

For triggered modes, in contrast, the number of events per second sets an upper limit to the concentration of the samples. This maximum trigger rate in the fluorescence-triggered mode is sufficiently high to measure the size structure of most natural samples in a reasonable amount of time. In the side-scatter-triggered mode, in contrast, the trigger rate is so low that, even concentrating the sample to the limit, the processing time is too high; consequently, it is not the appropriate working mode to estimate the size structure of natural samples. The problem with the need to concentrate the sample, in addition to possible artefacts and damage to the cells, is that it is necessary to know beforehand the natural cell densities to determine the degree of sample concentration required (maybe using proxies such as fluorescence or transmittance from automatic sensors).

The discrete sampling rate in autoimage requires that the cell distribution must be homogeneous to obtain reliable results, so it is very important to stir carefully the sample before and during the analysis especially if it contains large cells. Also, many particles are cut in the images as they can be placed in any of the four borders of the photograph and a too high concentration can increase the probability of coincident counts (Buskey and Hyatt, 2006). In the fluorescence-triggered mode, the counting is not as dependent on the homogeneity of the sample as in autoimage. Coincidence counting is unusual if the factory-defined limits regarding cell density are followed. Also, particles are captured preferably in the middle of the field-of-view so they can only be cut in the left and right borders of the image.

Depending on the study aim, it might be also necessary to analyse several subsamples each with a different working mode. For instance, if the aim is to distinguish autotrophic from heterotrophic organisms, and since autoimage and fluorescence-triggered modes cannot work together given their different designs, the only option would be to activate side-scatter and fluorescence together to count every particle differentiating the fluorescent ones. However, then the sample has to be processed within the strict analysing time limitations imposed by the side-scatter mode (Fig. 4F). Besides, some heterotrophic organism can have a fluorescence signal due to gut contents. In summary, to estimate the size spectrum of a natural sample, differentiating autotrophic and heterotrophic individuals could take a prohibitive amount of time, if the experimental protocol is not planned very carefully and taking the limitations of the instrument into account. Another option is to use only autoimage mode and try to classify the FlowCAM images in taxonomic or functional groups. This classification can be done *a posteriori* through visual inspection of the images, but it is time-consuming. Alternatively, the images can be classified automatically using classification algorithms (Blaschko *et al.*, 2005).

If FlowCAM can reproduce accurately the size structure of natural samples, at least working in autoimage and fluorescence-trigger modes, the next question is whether it can work with preserved samples. Our results show that there are not major differences between the size spectra obtained with FlowCAM and with light microscopy for preserved samples. It must be noted, however, that the size range each method can sample effectively is different. To cover the size range between 3 and 100 μm, both methods need to combine at least two magnifications. The lower size limit of the ×100 magnification in FlowCAM is 15 μm which requires that the ×200 magnification samples from 3 to 15 μm. In the microscope, the lower limit of the ×100 magnification is around 10 μm and the volume sampled with the ×200 is larger than in the FlowCAM (Table IV), so it is easier to sample the complete size spectrum with the traditional microscopy method.

The FlowCAM tends to underestimate the cell abundance in the size classes close to the upper size limit of the magnification/flow chamber. This underestimation of large cells can be caused by obstruction of the flow chamber. Cell clumping was not a problem with the cultures in Experiments 1 and 2 because cells are all elliptical without spines or chaetae, but it can be a problem in natural samples, where clumped cells can cause underestimation of cell abundance or even obstruction of the flow chamber. This effect is greater in preserved samples where cells tend to form aggregates larger than the flow-chamber depth (Zarauz and Irigoien, 2008).

Therefore, and considering all their limitations, the size-spectrum estimates obtained with FlowCAM can be as valid as the estimates obtained with microscope, but the time spent with each methodology is very different. FlowCAM can be slow, as we have shown previously, and can take a couple of hours to estimate the size spectrum of a sample over a wide size range, but to do exactly the same task, that is, count and size every particle, with a microscope can take more than a day. If the aim of the study is not size structure but simple enumeration, the microscope can be competitive in terms of time with FlowCAM (Littman *et al.*, 2008).

The size structure of preserved samples can be different to the size spectra of fresh samples (Zarauz and Irigoien, 2008). There are two effects causing this change, the different preservation response of organisms to fixation and the different effect of shrinkage (Leakey *et al.*, 1994; Menden-Deuer *et al.*, 2001). The decrease in the intercept and slope suggests a degradation of small cells due to a lack of rigid structures or a strong shrinkage what might cause the size of these particles to fall below the detection limit (James, 1991). The decrease in the slope can also be due to a disintegration of larger cells (Zarauz and Irigoien, 2008). This implies that the results from size-structure studies based on preserved samples, although correctly estimated, must be considered with caution, because they might not be showing the actual size structure of the community. If the actual size structure of the community can only be described with fresh samples, automatic sampling methods like FlowCAM are not only a faster alternative to traditional methods but the only choice. To be used in routine work, it is necessary that the device is highly robust or, at least, that there is a low incidence of mechanical failure, which, from our experience, may not always be the case with the present design of FlowCAM. For instance, during our experiments, we have experienced malfunction in the fluorescence and side-scatter detectors that have required shipment of the instrument back to the manufacturer for fixing. This has been the case with three FlowCAM devices our lab has worked with.

SUMMARY AND CONCLUSIONS

The inverse relationship between size and abundance in nature determines the sampling techniques used to estimate the size structure of the planktonic community. Automatic sampling devices must be capable of analysing a sufficient number of cells within a size range to ensure the representation of the largest/scarcest particles

of the range. We provide an analysis which allows the estimation of the volume or total number of particles that have to be counted to obtain a representative sample of the size spectrum. Some automatic devices, like the FlowCAM, have characteristic flow and particle detection systems which impose limits to the concentration of the samples to be processed leading to important constraints on the size range that can be effectively sampled in a given amount of time. Thus, the analysis of the size structure of natural samples with FlowCAM requires a planned pre-processing of the samples.

The side-scatter-triggered mode can count accurately a sparse solution of particles, but it has an analysis rate that is too low to estimate the size structure of natural samples. In contrast, autoimage and fluorescence-triggered modes cannot only count a mono-specific solution of cells accurately but can also estimate the size structure of natural samples. However, the requirements of each working mode in terms of sample concentration are different so the concentration procedure should be carefully chosen and some *a priori* knowledge about the cell density in the sample is needed.

The size structure obtained with FlowCAM and with light microscopy on preserved samples coincides but they differs from the size structure obtained on fresh samples. This suggests that automatic sampling devices could provide a more precise vision of plankton community avoiding the effects of sampling preservation and storage and increasing the resolution of the surveys.

SUPPLEMENTARY DATA

Supplementary data can be found online at http://plankt.oxfordjournals.org.

ACKNOWLEDGEMENTS

This is a contribution to SCOR Working Group 130 on Automatic Visual Plankton Identification. We are indebted to all components of the Red Tides and Harmful Algae team of the Centro Oceanográfico de Vigo (IEO) for their help at the laboratory and the access to the Toxic Phytoplankton Culture Collection. We thank the captain and crew in the R/V Thalassa for their assistance during the Pelacus1009 cruise.

FUNDING

This work was supported by the Plan de Ciencia, Tecnología e Innovación del Gobierno del Principado de Asturias (project IMAGINA and research grant BP07-081 to E.A.) and the Ministerio de Ciencia e Innovación (project PERPLAN, CTM2006-04854).

REFERENCES

Babin, M., Cullen, J. J., Roesler, C. *et al.* (2005) New approaches and technologies for observing harmful algal blooms. *Oceanography*, **18**, 210–227.

Barofsky, A., Simonelli, P., Vidoudez, C. *et al.* (2010) Growth phase of the diatom *Skeletonema marinoi* influences the metabolic profile of the cells and the selective feeding of the copepod *Calanus* spp. *J. Plankton Res.*, **32**, 263–272.

Bauman, A. G., Burt, J. A., Feary, D. A. *et al.* (2010) Tropical harmful algal blooms: an emerging threat to coral reef communities? *Mar. Pollut. Bull.*, doi: 10.1016/j.marpolbul.2010.08.015.

Benfield, M. C., Grosjean, P., Culverhouse, P. *et al.* (2007) RAPID: research on automated plankton identification. *Oceanography*, **20**, 12–26.

Blanco, J. M., Echevarría, F. and García, C. M. (1994) Dealing with size-spectra: some conceptual and mathematical problems. *Sci. Mar.*, **58**, 17–29.

Blaschko, M. B., Holness, G., Mattar, M. A., Lisin, D., Utgoff, P. E., Hanson, A. R., Schultz, H., Riseman, E. M., Sieracki, M. E., Balch, W. M. and Tupper, B. (2005) Automatic in situ identification of plankton. *Proceedings of the Seventh IEEE Workshops on Application of Computer Vision (WACV/MOTION'05)*, **1**, 79–86.

Breier, C. F. and Buskey, E. J. (2007) Effects of the red tide dinoflagellate, *Karenia brevis*, on grazing and fecundity in the copepod *Acartia tonsa*. *J. Plankton Res.*, **29**, 115–126.

Brown, L. (2010) *Using Laser-scatter Triggering in an Imaging Particle Analysis System to Increase Particle Counting Accuracy in Sparse Samples*. Fluid Imaging Technologies, Yarmouth, ME, 8 pp.

Brzezinski, M. A., Baines, S. B., Balch, W. M. *et al.* (2010) Co-limitation of diatoms by iron and silicic acid in the equatorial Pacific. *Deep-Sea Res. II*, doi: 10.1016/j.dsr2.2010.08.005.

Buskey, E. J. (2008) How does eutrophication affect the role of grazers in harmful algal bloom dynamics? *Harmful Algae*, **8**, 152–157.

Buskey, E. J. and Hyatt, C. J. (2006) Use of the FlowCAM for semi-automated recognition and enumeration of red tide cells (*Karenia brevis*) in natural plankton samples. *Harmful Algae*, **5**, 685–692.

Clough, J. and Strom, S. (2005) Effects of *Heterosigma akashiwo* (Raphidophyceae) on protist grazers: laboratory experiments with ciliates and heterotrophic dinoflagellates. *Aquat. Microb. Ecol.*, **39**, 121–134.

Cotano, U., Irigoien, X., Etxebeste, E. *et al.* (2008) Distribution, growth and survival of anchovy larvae (*Engraulis encrasicolus* L.) in relation to hydrodynamic and trophic environment in the Bay of Biscay. *J. Plankton Res.*, **30**, 467–481.

Dodson, A. N. and Thomas, W. H. (1978) Reverse filtration. In Sournia, A. (ed.), *Phytoplankton Manual*. UNESCO, Paris, pp. 104–107.

Gribben, P. E., Wright, J. T., O'connor, W. A. *et al.* (2009) Reduced performance of native infauna following recruitment to a habitat-forming invasive marine alga. *Oecologia*, **158**, 733–745.

Haury, L. R., Mcgowan, J. A. and Wiebe, P. H. (1978) Patterns and processes in the time-space scales of plankton distributions. In: Steele, J. H. (ed.), *Spatial Pattern in Plankton Communities*. Plenum Press, New York, pp. 277–327.

Ide, K., Takahashi, K., Kuwata, A. *et al.* (2008) A rapid analysis of copepod feeding using FlowCAM. *J. Plankton Res.*, **30**, 275–281.

James, M. R. (1991) Sampling and preservation methods for the quantitative enumeration of microzooplankton. *N. Z. J. Mar. Fresh.*, **25**, 305–310.

Koski, M., Breteler, W. K., Schogt, N. *et al.* (2006) Life-stage-specific differences in exploitation of food mixtures: diet mixing enhances copepod egg production but not juvenile development. *J. Plankton Res.*, **28**, 919–936.

Kudela, R. M., Lane, J. Q. and Cochlan, W. P. (2008) The potential role of anthropogenically derived nitrogen in the growth of harmful algae in California, USA. *Harmful Algae*, **8**, 103–110.

Lavrentyev, P. J., Mccarthy, M. J., Klarer, D. M. *et al.* (2004) Estuarine microbial food web patterns in a Lake Erie coastal wetland. *Microbial. Ecol.*, **48**, 567–577.

Leakey, R. J. G., Burkill, P. H. and Sleigh, M. A. (1994) A comparison of fixatives for the estimation of abundance and biovolume of marine planktonic ciliate populations. *J. Plankton Res.*, **10**, 375–389.

Littman, R. A., Van Oppen, M. J. H. and Willis, B. L. (2008) Methods for sampling free-living *Symbiodinium* (zooxanthellae) and their distribution and abundance at Lizard Island (Great Barrier Reef). *J. Exp. Mar. Biol. Ecol.*, **364**, 48–53.

Liu, H., Dagg, M. J. and Strom, S. (2005) Grazing by the calanoid copepod *Neocalanus cristatus* on the microbial food web in the coastal Gulf of Alaska. *J. Plankton Res.*, **27**, 647–662.

Menden-Deuer, S., Lessard, E. J. and Satterberg, J. (2001) Effect of preservation on dinoflagellate and diatom cell volume and consequences for carbon biomass predictions. *Mar. Ecol. Prog. Ser.*, **222**, 41–50.

Nielsen, L. T., Jakobsen, H. H. and Hansen, P. J. (2010) High resilience of two coastal plankton communities to twenty-first century seawater acidification: evidence from microcosm studies. *Mar. Biol. Res.*, **1**, 1–14.

Pedersen, T. M., Almeda, R., Fotel, F. L. *et al.* (2010) Larval growth in the dominant polychaete *Polydora ciliata* is food-limited in a eutrophic Danish estuary (Isefjord). *Mar. Ecol. Prog. Ser.*, **407**, 99–110.

Reynolds, R. A., Stramski, D., Wright, V. M. *et al.* (2010) Measurements and characterization of particle size distributions in coastal waters. *J. Geophys. Res.*, **115**, doi: 10.1029/2009JC005930.

San Martin, E., Harris, R. P. and Irigoien, X. (2006a) Latitudinal variation in plankton size spectra in the Atlantic Ocean. *Deep-Sea Res. II*, **53**, 1560–1572.

San Martin, E., Irigoien, X., Harris, R. P. *et al.* (2006b) Variation in the transfer of energy in marine plankton along a productivity gradient in the Atlantic Ocean. *Limnol. Oceanogr.*, **51**, 2084–2091.

See, J. H., Campbell, L., Richardson, T. L. *et al.* (2005) Combining new technologies for determination of phytoplankton community structure in the northern Gulf of Mexico. *J. Phycol.*, **41**, 305–310.

Sheldon, R. W., Prakash, A. and Sutcliffe, W. H. Jr. (1972) The size distribution of particles in the ocean. *Limnol. Oceanogr.*, **17**, 327–340.

Sieracki, C. K., Sieracki, M. E. and Yentsch, C. S. (1998) An imaging-in-flow system for automated analysis of marine microplankton. *Mar. Ecol. Prog Ser.*, **168**, 285–296.

Sterling, M. C. Jr., Bonner, J. S., Ernest, A. N. S. *et al.* (2004) Characterizing aquatic sediment-oil aggregates using in situ instruments. *Mar. Pollut. Bull.*, **48**, 533–542.

Tanoi, T., Kawachi, M. and Watanabe, M. M. (2010) Effects of carbon source on growth and morphology of *Botryococcus braunii*. *J. Appl. Phycol.*, doi: 10.1007/s10811-010-9528-4.

Tauxe, L., Steindorf, J. L. and Harris, A. (2006) Depositional remanent magnetization: toward an improved theoretical and experimental foundation. *Earth Planet. Sci. Lett.*, **244**, 515–529.

Töpper, B., Larsen, A., Thingstad, T. F. *et al.* (2010) Bacterial community composition in an Arctic phytoplankton mesocosm bloom: the impact of silicate and glucose. *Polar Biol.*, doi: 10.1007/s00300-010-0846-4.

Utermöhl, H. (1958) Zur Vervollkommnung der quantitativen Phytoplankton-Methodik. *Mitt. Int. Ver. Theor. Angew. Limnol.*, **9**, 1–38.

Vaillancourt, R. D., Brown, C. W., Guillard, R. R. L. *et al.* (2004) Light backscattering properties of marine phytoplankton: relationships to cell size, chemical composition and taxonomy. *J. Plankton Res.*, **26**, 191–212.

Zar, J. H. (1999) *Biostatistical Analysis*. Prentice-Hall, Englewood Cliffs, New Jersey.

Zarauz, L. and Irigoien, X. (2008) Effects of Lugol's fixation on the size structure of natural nano-microplankton samples, analyzed by means of an automatic counting method. *J. Plankton Res.*, **30**, 1297–1303.

Zarauz, L., Irigoien, X. and Fernandes, J. A. (2009) Changes in plankton size structure and composition, during the generation of a phytoplankton bloom, in the central Cantabrian sea. *J. Plankton Res.*, **31**, 193–207.

Zarauz, L., Irigoien, X., Urtizberea, A. *et al.* (2007) Mapping plankton distribution in the Bay of Biscay during three consecutive spring surveys. *Mar. Ecol. Prog. Ser.*, **345**, 27–39.